

Electronic, optical and charge transfer properties of topologically protected states in hybrid bismuthene layers

Erika Nascimento Lima

*Universidade Federal do Mato Grosso,
Campus Rondonópolis, Rondonópolis, Mato Grosso, Brazil*

Andreia Luisa da Rosa (ORCID: 0000-0002-2780-6448)

*Universidade Federal de Goiás, Institute of Physics,
74690-900 Goiânia, Goiás, Brazil and
Bremen Center for Computational Materials Science,
University of Bremen, Am Fallturm 1, 28359 Bremen, Germany*

Renato Borges Pontes (ORCID: 0000-0002-3336-3882)

Universidade Federal de Goiás, Institute of Physics, 74690-900 Goiânia, Goiás, Brazil

Tome Mauro Schmidt

*Universidade Federal de Uberlândia, Institute of Physics,
38400-902 Uberlândia, Minas Gerais, Brazil*

Jailton Almeida

Universidade Federal da Bahia, Institute of Physics, 40210-340 Salvador, Bahia, Brazil

Thomas Frauenheim (ORCID: 0000-0002-3073-0616)

*Bremen Center for Computational Materials Science,
University of Bremen, Am Fallturm 1, 28359 Bremen, Germany*

Maurício Chagas da Silva (ORCID: 0000-0002-6890-0182)

*Max-Planck-Institute for the Structure and Dynamics of Matter,
Luruper Chaussee 149, 22761 Hamburg, Germany and
Bremen Center for Computational Materials Science,
University of Bremen, Am Fallturm 1, 28359 Bremen, Germany*

Abstract

We have performed first-principles calculations of electronic and dielectric properties of single-layer bismuth (bismuthene) adsorbed with -COOH. We show that the Bi-COOH hybrid structure is a two-dimensional topological insulator with protected edge Dirac states. The adsorption process of -COOH induces a planar configuration to the initially pristine buckled bismuthene. We claim that the stability of these planar structure mainly stem from strain induced by the adsorption of the -COOH organic group, but it is also related to ligand-ligand interactions. Using charge density analysis we show that the role of this organic group is not only to stabilize the layer but also to functionalize it, which is very important for future applications such as sensing, biomolecules immobilization, as well in electronic spintronic and even optical devices, due to its large band gap. Finally we demonstrate that many body corrections are crucial to obtain a better description of the electronic and dielectric properties of these systems.

I. INTRODUCTION

Bismuth single layers were theoretically predicted to have topological insulator behavior with protected edge non-trivial Dirac states [1–3], which are robust against perturbations that preserve time reversal symmetry, like strain and external electric field [4]. Only recently the existence of pure, ultra-thin bismuth layers has been experimentally confirmed, which were synthesized on a silicon carbide substrate [5]. Although bismuthene has already inherent properties such as topological non-trivial band structure, it has been proposed that these bismuth layers are very sensitive to changes in the environment [2, 6].

A promising route for tuning the electronic properties of bare layered materials is the adsorption of organic functional groups [7]. Previously, -H and $-\text{CH}_3$ groups have been investigated. Both groups were predicted to preserve the topological insulator behavior of bismuthene [1, 2]. Furthermore, valley-polarized quantum anomalous Hall states emerge as these bismuth layers films are adsorbed with hydrogen [8], enlarging the band gap, indicating that ligand-mediated interactions with the substrate may be a route to functionalize this 2D TI. More recently it has been proposed that -COOH groups can induce ferroelectric behavior on bismuthene layers [6]. Theoretical calculations of optical properties of a single-layer bismuthene have been recently reported by Kecik *et al.* [9]. In such investigation, an exciton with binding energy of 0.18 eV has been found, with a strong absorption peak around 2.2 eV, indicating that such 2D material can be useful for applications, in solar cells, light-emitting devices, photodetectors, among others.

Despite all that, the role of organic ligands on bismuthene on introducing new functionalities, such as change of reactivity, which is a requirement for further applications such as immobilization of organic or biomolecules and also in the field of catalysis, has been little discussed. Furthermore, dielectric and optical properties of hybrid bismuthene-organic systems remain unexplored.

In this work, we employ density-functional theory (DFT) and many-body theory (GW) to show that the bismuthene-based hybrid structures preserve the topological insulating behavior. We show that the adsorption of -COOH groups induces a planar geometry on the initially buckled bismuthene structure. Most importantly our results reveal that the role of -COOH groups is not only to protect the 2D layer but also to functionalize the bismuth layers by changing the reactivity of the hybrid system. Furthermore we perform GW calculations

to obtain the electronic band gap and dielectric properties of the hybrid layers. We find that self-consistency in the GW calculations is necessary to obtain a better description of the dielectric properties compared to single-shot GW calculations. Finally, we suggest that the charge transfer between the ligand and the bismuth layer promoted by adsorption is important for future applications such as sensing and biomolecules immobilization.

II. METHODOLOGY

The electronic structure and the chemical bond analysis of bismuthene adsorbed with -COOH groups were investigated within density functional theory framework. The projected augmented wave method (PAW) [10, 11] combined with the generalized gradient approximation [12] as implemented in the VASP package has been employed [11, 13]. The lattice parameters and atomic position were fully relaxed until the atomic forces converge to less than 10^{-4} eV/Å. A vacuum region of at least 10 Å perpendicular to the bismuth surface was introduced to avoid interaction between atoms in neighboring cells. The reciprocal space was sampled with a $(10 \times 10 \times 1)$ \mathbf{k} -point Γ -centered grids to relax the structures. The wave functions were expanded in a plane-wave basis set with an energy cutoff of 500 eV. Spin orbit coupling (SOC) was included in all calculations, including relaxation, electronic structure and dielectric properties. The dielectric function was calculated using the GW approximation with 8 iterations in the Green's function G , which was found to be sufficient enough to converge the quasi-particle eigenvalues with respect to G_0W_0 calculations. In the later case, a $(5 \times 5 \times 1)$ \mathbf{k} -point grid was used due to the high computational costs. Tests with up to a $(12 \times 12 \times 1)$ \mathbf{k} -points for bare single-layered bismuth have shown that this smaller set is enough to achieve convergence. Moreover, due to high computational cost the energy cutoff for GW calculations has been decreased to 400 eV.

III. RESULTS AND DISCUSSION

The stability of the pristine buckled and the planar bismuthene has been investigated by varying the lattice parameters a and b and fully relaxing all the atoms in the unit cell. The optimized in-plane lattice parameters are $a = b = 4.39$ Å for the buckled structure and $a = b = 5.30$ Å for the planar one. Our results are in good agreement with the results obtained by

Freitas et al. [2], whose DFT-based calculations indicate that buckled bismuthene exhibits an equilibrium structure with a buckling parameter $\Delta = 1.73 \text{ \AA}$ and a lattice constant $a = 4.34 \text{ \AA}$. For a planar bismuthene they obtained a lattice constant $a = 5.57 \text{ \AA}$. Our calculated structural parameters for buckled bismuthene are also in very good agreement with previous theoretical and experimental values in the literature [14–18].

The inclusion of SOC does not change significantly the lattice parameters, but it lowers the total energy of the system. We found that the buckled structure is much more stable than the planar configuration with an energy difference of 1.55 eV. The electronic stability of the buckled structure compared to the planar one can be understood considering that in two-dimensional bismuthene each bismuth atom has three nearest neighbors forming σ -like bonds. In order to achieve the electronic stability, the sp^3 hybridization is favored in respect to the planar sp^2 -type hybridization, leading to a buckled structure. This structural configuration can be explained by the qualitative assumptions of the valence shell electron pair repulsion (VSEPR) theory [19]. The VSEPR theory suggests that the electronic density of molecules, localized bonds and/or lone electrons pairs, seeks for spatial configuration which minimizes the electron-electron interactions, i.e., the angles between the localized bonds and/or lone electrons pair should be greatest to minimize the repulsion between them in a such spatial arrangement. Thus, the sp^3 hybridization presents an angle of about 109° between the lone electrons pairs of Bi centers and the Bi-Bi σ bonds. This geometric arrangement has an angle which is larger than the 90° considering a sp^2 hybridization. This minimizes the electron-electron interactions between the Bi-Bi σ -like bond and the non-bonded lone electrons pairs of Bi centers producing a buckling of 1.72 \AA . In this configuration, bismuthene has a band gap of 0.9 eV, in good agreement with previously reported results [2, 6].

In this investigation, we have adsorbed -COOH on bismuthene at one monolayer (ML) coverage regime. The ligands are adsorbed on top positions of bismuth atoms on both sides of the bismuth surface. We verified that the configurations where the radicals are on top positions are more stable than hollow or bridge sites. Although, we cannot rule out that smaller coverages may be present, we should point out that lower coverages were found to yield less stable structures in other two-dimensional hybrid systems, such as germanene [20].

Fig. 1 shows a side view of relaxed hybrid bismuthene-COOH layer. Upon adsorption of -COOH group, the initial buckled geometry of bismuthene relaxes to a near planar structure,

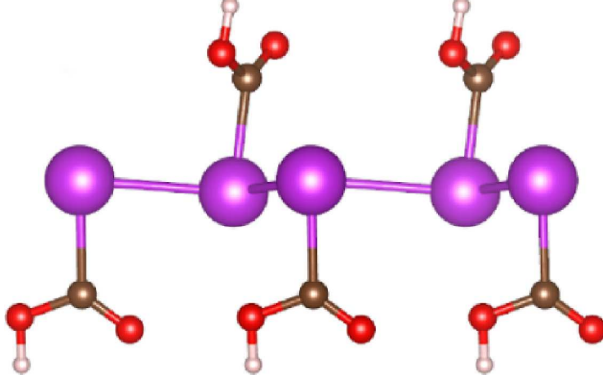


FIG. 1. (color online) Side view of bismuth layer adsorbed with $-\text{COOH}$ at 1 ML coverage regime.

with an in-plane lattice parameter of 5.10 \AA . There are two main driving forces for the planarity of these structures: the ligand-ligand interaction and the electronegativity of the ligand. Again, according to the VSERP theory [19], the sp^3 hybridization should be preferred in the adsorbed layers against the sp^2 in bare bismuthene. However, lateral ligand-ligand interactions play an important role as well. As a consequence of these additional ligand-ligand interactions, the system assumes a quasi-planar configuration which increases the in-planar lattice constant. The hybrid system then assumes a quasi-planar arrangement in which the Bi-Bi bonds are larger compared to pure bismuthene and Bi-Bi-C angle is reduced to almost 90° in a sp^3 hybridization, as shown in Fig. 1. A similar behaviour has been suggested for organic functionalized germanene [20].

In the absence of SOC, Bi-COOH exhibits semi-metallic character and fourfold degeneracy at the Γ point. From the orbital projected band structure in Fig. 2 (a) and (b), one can see that the p_x , p_y and p_z orbitals dominate the bands near the Fermi level, mainly coming from Bi atoms. The change in the geometry and inclusion of SOC upon -COOH adsorption shown in Fig. 2 (c) and (d) shifts the conduction band minimum (CBM) from K to Γ . We can see some contributions from the -COOH group at valence band maximum (VBM) and conduction band minimum (CBM). An indirect band gap is found since the VBM is at the K point and the CBM lies at the Γ point. The resulting indirect band gap of 1.0 eV is 10% larger than the bare bismuthene band gap. It is also possible to identify further transitions of 2.0 eV at Γ , 3.2 eV at M and 1.1 eV at K points. This is similar to what has been reported in H and CH_3 adsorbed on bismuth layers [1, 2, 21] using GGA calculations. One can see that most p_x and p_y orbitals belonging to bismuth contribute to states close to Fermi level.

Molecular states also lie close to Fermi level. The CBM contains both p_x and p_y characters of bismuth and ligand. As a conclusion, the hybrid systems contain significant contribution from both bismuth and ligand orbitals. However, the interaction between ligands at such a high coverage induces strain, which weakens the Bi-Bi bonds, as discussed above. Although this effect makes the planar bonds larger, the bismuth-ligand interaction is strong enough to stabilize the hybrid layers. This will be discussed below, as there is a net charge accumulation of electrons on the ligand oxygen atom. We should mention that electrons s do not contribute to states close to the Fermi level, since they appear far below in energy from the top of the valence band.

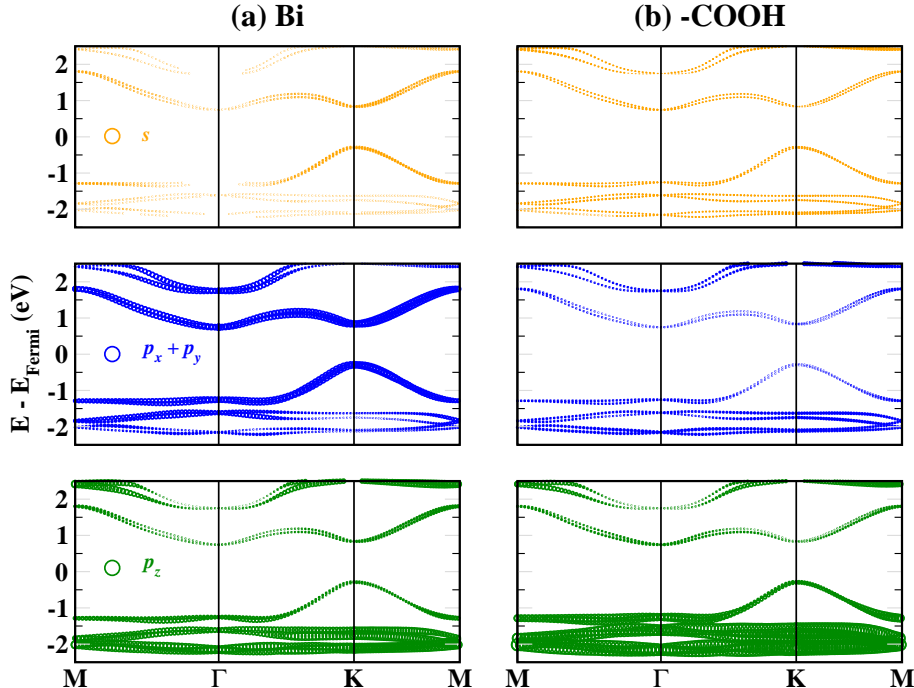


FIG. 2. Projected band structures on p_x (blue), p_y (red) and p_z (orange) orbitals. Without the inclusion of SOC project: a) on bismuth and b) on ligand atoms. And with the inclusion of SOC projected on c) on bismuth and d) on ligand atoms. The Fermi level is set to zero energy in all plots.

In addition we show the projected density of states (PDOS) on the individual atoms in Fig. 3. The atomic orbital interpretation of the bands close to the Fermi level can be split into two main energetic range regions, namely Φ_1 and Φ_2 , shown in the inset of Fig. 3 (c). We can see that the contribution of the carbon orbitals are very small compared to the

bismuth and oxygen atoms in both Φ_1 and Φ_2 regions. Moreover, the σ -like bond between Bi-C has a large contribution of the bismuth p_z orbitals with a large electron donation to carbons atoms. In this scenario, the bismuth atoms act as a Lewis basis donating electronic density through the σ bond. On the other hand, the carbon atoms act as a Lewis acid receiving electronic density from the bismuth atoms via the σ bond.

The Bi-C σ -like bond is better represented by the Φ_2 energetic band region shown in Fig. 3. The Φ_1 region is majority Bi-Bi bonds which can be interpreted as a combination of the in-plane orbitals, p_x and p_y orbitals. The Φ_1 region contemplates the top of the VB region, and so it dictates the band gap behavior. As we can see from the charge density in Fig. 3, Φ_1 comes mostly from the in-plane Bi-Bi (p_x, p_y) bonds. So, the increase in the band gap of the Bi-COOH with respect to the bare bismuthene must be due to the flattening Bi-Bi bonds. The Φ_2 region is mostly associated to Bi-C σ -like bond as it can be seen in Fig. 3. The main frontier bands of Bi-COOH is basically formed by Bi-Bi bonds with delocalized orbitals, which can be explained by the composition of p_x and p_y Bi orbitals. Moreover, the Bi-C bond lies also deeper inside the valence band demonstrating in fact the presence of a Bi-C bond.

The nature of the chemical bonds in the hybrid system was investigated by the charge density difference between the electronic densities of the Bi-COOH and their constituent systems. The electronic density difference ($\Delta\rho$) is given by: $\Delta\rho = \rho^{\text{Bi-COOH}} - \rho^{\text{Bi}} - \rho^{-\text{COOH}}$, where $\rho^{\text{Bi-COOH}}$ is the electronic density of the hybrid Bi-COOH layers, ρ^{Bi} and $\rho^{-\text{COOH}}$ are the charge densities calculated at fixed atomic positions of the Bi and -COOH, respectively. The charge density difference shown in Fig. 4 reflects on how the electronic charge density changes upon -COOH adsorption. The complex Bi-COOH has a high electronic density between Bi-C atoms. It is also seen that the electronic charge density accumulates half-way of the bond regions, decreasing the electronic density around the atomic regions (shown in blue). The Bi-Bi bond suffer small changes, while a strong Bi-C bond can be seen in Fig. 4-b. Since upon cleavage of the bulk (111) surface the bismuth atoms are left with two extra electrons on the unsaturated bonds, upon -COOH adsorption covalent bonds between C and Bi bonds are expect to form. We can also notice that the charge is further distributed to the oxygen atoms on the ligand (O1 and O3). This is an important conclusion, since it reveals that the role of -COOH is not only to protect the Bi surface, but also to functionalize the bismuth layers.

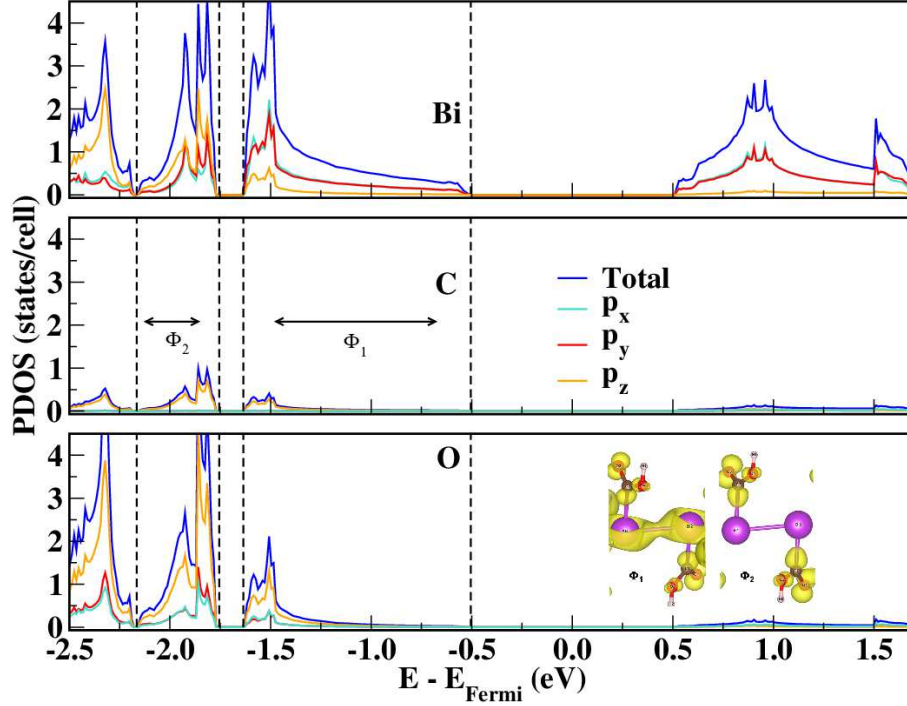


FIG. 3. Total charge density showing the regions Φ_1 and Φ_2 and orbital resolved projected density of states for monolayer Bi-COOH. The Fermi level is set at zero energy in all plots. The insets stand for charge density plots of the regions Φ_1 and Φ_2 , respectively. The Fermi level is set at zero.

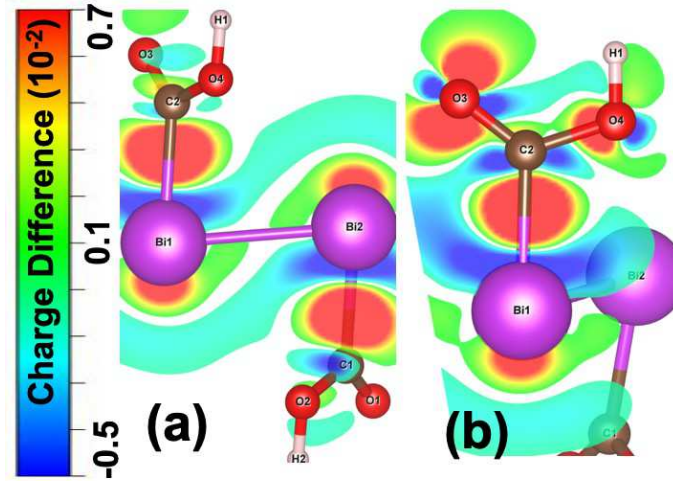


FIG. 4. Two views of the charge density difference ($\Delta\rho$) for monolayer Bi-COOH. Negative (positive) values represent regions where electrons were accumulated (withdrawn) after adsorption.

In order to have insight on the nature of the chemical bond environment in the functionalized Bi-COOH system, the electronic localization function (ELF) [22] was also evalu-

ated. ELF represents the electronic density localization in the spatial region of crystals and molecules, whose values vary between 0 to 1. ELF values about 0.5 can be interpreted as metallic type bonds (green in Fig. 5), whereas values close to 1.0 indicate localized electronic densities (covalent bonds between atoms or a non-bonding lone electron pairs, shown in red color in Fig. 5)). The ELF of the Bi-COOH, Bi-buckled and Bi-planar are presented in Fig. 5. In Fig. 5(a), a region of localized electronic density between carbon and bismuth atoms can be clearly identified (ELF values close to 1.0), thus characterizing a covalent bond. In addition, it is possible to see that the C-Bi chemical bond has a slight ionic characteristic which is usual for -COOH groups. The low electronic charge density between the bismuth atoms is also verified for the Bi-planar structure, shown in Fig. 5(c). However, in the Bi-buckled structure, the ELF reveals a metallic bond nature between Bi bonds, 5(b). The formation of the Bi-COOH bonds induced a distortion into the geometry from a chair-like configuration in Bi-buckled to a planar configuration. The chemical behavior of -COOH group withdraws electronic density of the Bi atoms, which it contributes to the reduction of the electronic density along Bi-Bi bonds. We can then conclude that the adsorption of -COOH groups change not only the geometrical feature of bismuthene, but also introduces a charge transfer between the ligand and the bare bismuth layers and therefore a change in the reactivity.

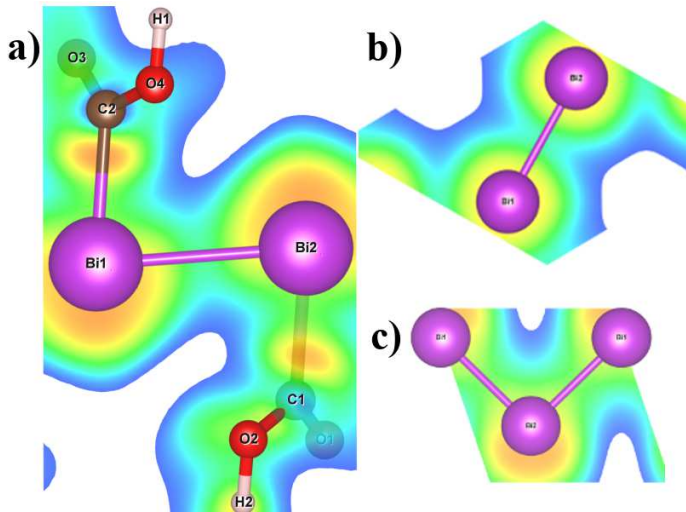


FIG. 5. (a-c) Different views of the electronic localization function cross-section for a single-layer Bi-COOH. The metallic feature of bismuth bonds is shown in green. The localized regions due to covalent bonds and lone-pair electrons of non-bonding orbitals are shown in orange.

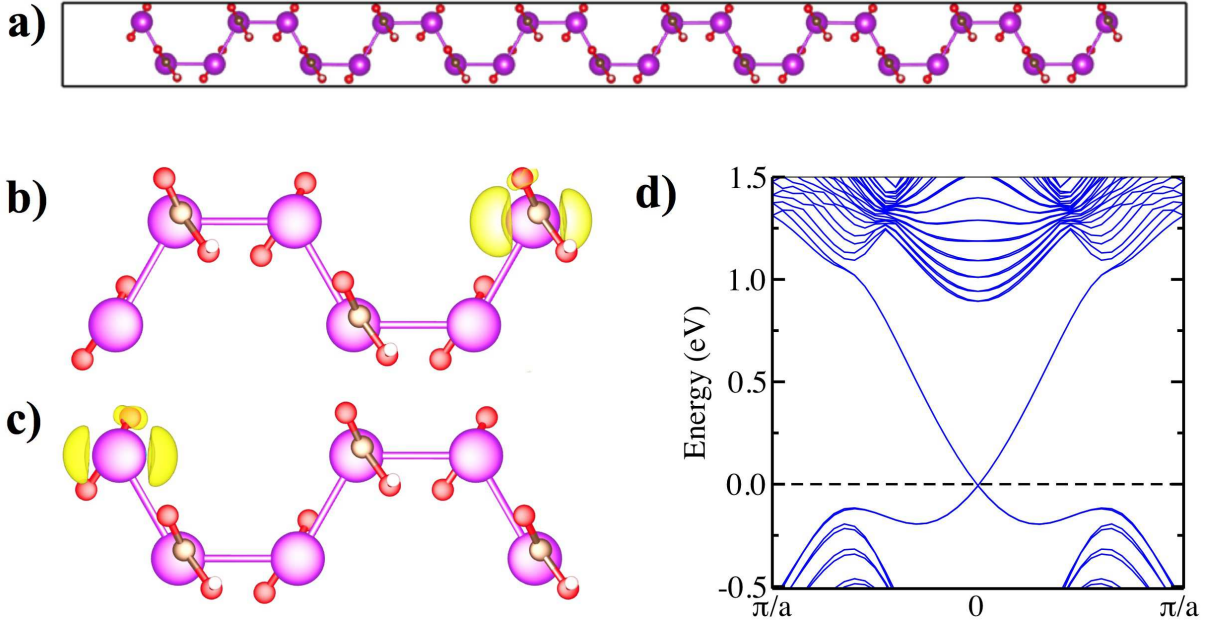


FIG. 6. a) DFT-GGA relaxed geometry of the Bi-COOH nanoribbon, b) band decomposed charge density at Γ point (spin up), c) band decomposed charge density at Γ point (spin down) and d) electronic band structure of a Bi-COOH nanoribbon. The optimized in-plane lattice parameters are: $a = 5.5 \text{ \AA}$ and $b = 63.55 \text{ \AA}$. The Fermi level is set at zero. Isosurface value is set to 0.002 e/\AA^3 .

The question that rises now is whether the hybrid system have a topologically nontrivial band structure. We have calculated the Z_2 topological invariant according to xx. This number corresponds to the number of Kramers pairs of edge modes, integrating over half of the Brillouin zone. If the overall Z_2 sum of occupied bands is even, the system is a regular insulator. On the other hand, if the sum is odd, the system is a topological insulator. We find that Z_2 is equal to 1, which means that the hybrid Bi-COOH layres behave as topological insulator. Additionally, we have calculated the band structure of a bismuth nanoribbon with zig-zag edges adsorbed with -COOH, as shown in Fig. 6 (a). Once the edges are exposed, it is possible to verify whether the topological states come from the edge atoms. The Bi-COOH nanoribbons contain 28 Bi atoms, 28 C atoms, 56 O atoms and 28 H atoms and have width of 60 \AA , which suffices to avoid spurious interaction between two edge-ends (a ribbon with 102 \AA width leads to identical results). Figs. 6 (a) and (b) shows the band projected electronic charge density at the Γ point for the edge states. It is clearly seen that the spin up, Fig. 6 (b) and spin down Fig. 6 (c) states are very localized at the edges only, confirming

a non-trivial character of the band structure. The calculated electronic band structure of the functionalized nanoribbon is shown in Fig.6 (d). One can see the topological edge states with a single Dirac crossing at M points, confirming that the edge states are protected by time reversal symmetry. Since the band gap of the hybrid Bi-COOH is enlarged with respect to bare bismuthene, optical applications can be important in this 2D TI material. Besides that Bi 5d orbital is completely filled, and many-body effects are expected to be significant [9]. Thus, we have calculated the dielectric function (ϵ). In particular, we computed the imaginary term of the electronic dielectric function (ϵ_2) for the Bi-COOH hybrid system within both the independent particle (IPA) and GW approximations. The ϵ_2 is shown in Fig.7. The inclusion of SOC in the optical properties is also taken into account. Both IPA, Fig.7(a), and GW, Fig.7(b), approximations show an anisotropic behaviour. In the IPA, an intense absorption band around 2.1 eV is seen for the averaged $(\epsilon_2^{xx} + \epsilon_2^{yy})/2$ parallel component. On the other hand, the ϵ_2^{zz} component is broadly distributed in the region 0-10 eV. In the IPA, the electronic (indirect) band gap is 1.0 eV, which correspond to the onset seen Fig.7(a). The inclusion of many-body effects in the G_0W_0 approximation, i.e., without self-consistency neither in the Green's function G nor in the screened Coulomb potential W, improves the electronic band gap a little to 1.01 eV. However, self-consistency in G gives a value of 2.4 eV to the band gap of the hybrid Bi-COOH, which is larger than the G_0W_0 value. This results is shown in Fig.7(b). The first strong transition is around 3 eV. A large anisotropy is also seen. The ϵ_2^{zz} component is a broad function between 5 and 30 eV. Our results show that the inclusion of many-body effects are important to obtain a better description of the dielectric properties.

IV. CONCLUSIONS

We have performed density-functional theory and GW calculations of electronic and dielectric properties for bismuthene adsorbed with -COOH groups. The electronic properties of this hybrid system show that the functionalized layers have topological insulating behavior with a reasonable band gap. Our results reveal that the stability of these planar structure stem from both reactivity change induced by the adsorption of -COOH on the buckled bismuth layers promoting C-Bi bonds. Furthermore, the role of -COOH groups is to functionalize the bismuth layers, since oxygen atoms belonging to the ligand become

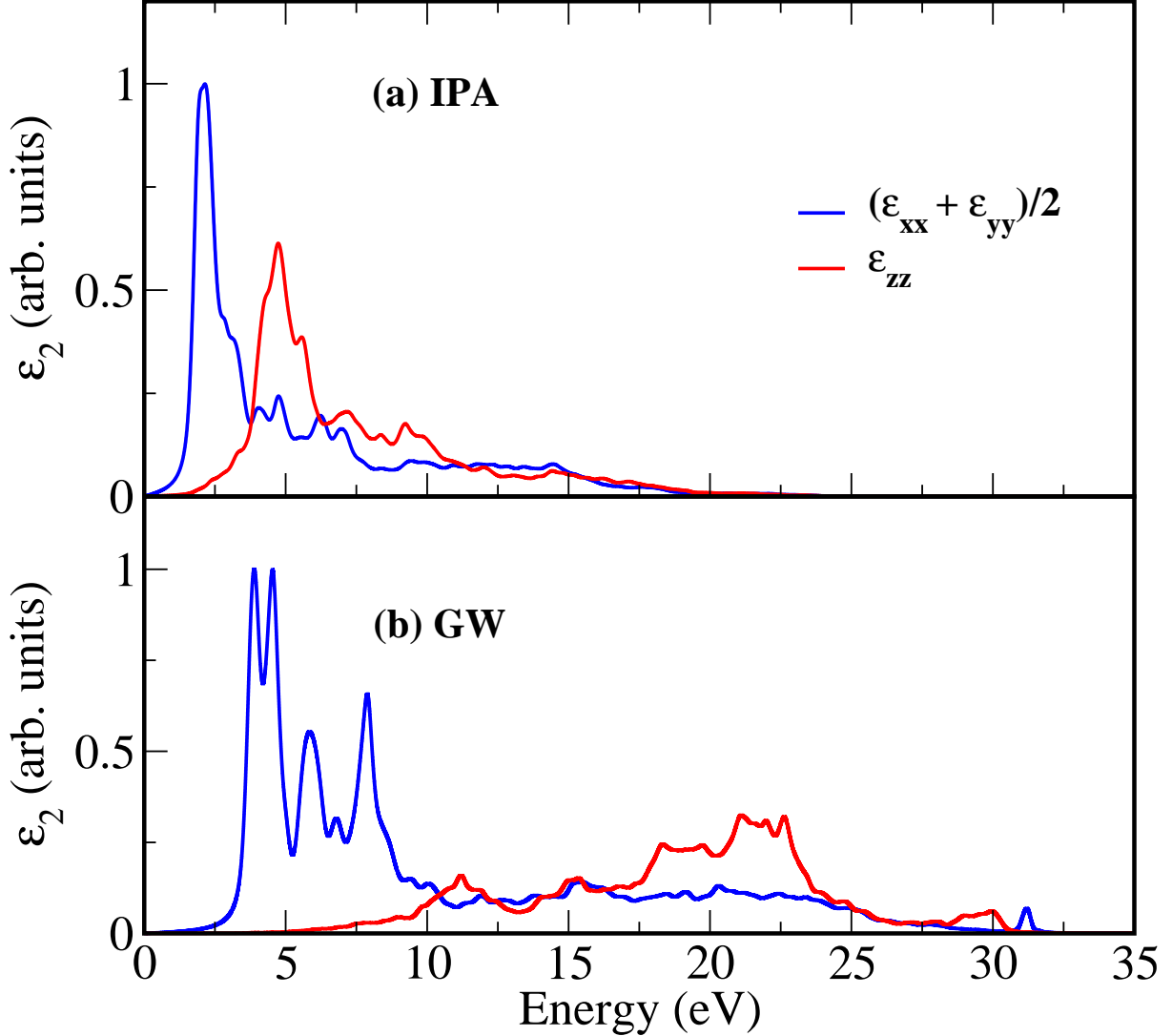


FIG. 7. Imaginary electronic dielectric function (ϵ_2) profile, for Bi-COOH system, in the: (a) independent particle approximation (IPA) and (b) GW approximation.

reactive. This reactivity is desired for enhanced catalysis or immobilization of organic and biomolecules. Finally we show that inclusion of many-body effects is very important to obtain a better description of the dielectric properties of the hybrid system compared to the independent particle approximation.

V. ACKNOWLEDGEMENTS

We acknowledge the financial support from the Brazilian Agencies CNPq and FAPEG (PRONEX 201710267000503) and German Science Foundation (DFG) under the program

FOR1616. The calculations have been performed using the computational facilities of CENAPAD-SP and LNCC (Supercomputer Santos Dumont) and at QM3 cluster at the Bremen Center for Computational Materials Science.

- [1] Y. Ma, Y. Dai, L. Kou, T. Frauenheim, and T. Heine, *Nano Letters* **15**, 1083 (2016), URL <https://doi.org/10.1021/nl504037u>.
- [2] R. R. Q. Freitas, R. Rivelino, F. de Brito Mota, C. M. C. de Castilho, A. Kakanakova-Georgieva, and G. K. Gueorguiev, *J. Phys. Chem. C* **119**, 23599 (2015), URL <https://doi.org/10.1021/acs.jpcc.5b07961>.
- [3] Z. Song, C.-C. Liu, J. Yang, J. Han, M. Ye, B. Fu, Y. Yang, Q. Niu, J. Lu, and Y. Yao, *NPG Asia Materials* **6**, e147 (2014), URL <https://doi.org/10.1038/am.2014.113>.
- [4] M.-Y. Liu, Y. Huang, Q.-Y. Chen, Z.-Y. Li, C. Cao, and Y. He, *RSC Advances* **7**, 3954639555 (2017), URL DOI:10.1039/C7RA05787C.
- [5] F. Reis, G. Li, L. Dudy, M. Bauernfeind, Glass, W. Hanke, R. Thomale, J. Schäfer, and R. Claessen, *Science* **357**, 287 (2017), URL [10.1126/science.aai8142](https://doi.org/10.1126/science.aai8142).
- [6] L. Kou, H. Fu, Y. Ma, B. Yan, T. Liao, A. Du, and C. Chen, *Phys. Rev. B* (2018), URL <https://doi.org/10.1103/PhysRevB.97.075429>.
- [7] Y. Ren, Z. Qiao, and Q. Niu, *Rep. Prog. Phys.* **79**, 066501 (2016), URL <https://doi.org/10.1088/0034-4885/79/6/066501>.
- [8] C. Niu, G. Bihlmayer, H. Zhang, D. Wortmann, S. Blügel, and Y. Mokrousov, *Phys. Rev. B* **91**, 041303 (2015).
- [9] D. Kecik, V. O. Özçelik, E. Durgun, and S. Ciraci, *Phys. Chem. Chem. Phys.* **21**, 7907 (2018).
- [10] P. E. Blöchl, *Phys. Rev. B* **50**, 17953 (1994), URL <http://link.aps.org/doi/10.1103/PhysRevB.50.17953>.
- [11] G. Kresse and D. Joubert, *Phys. Rev. B* **59**, 1758 (1999), URL <http://link.aps.org/doi/10.1103/PhysRevB.59.1758>.
- [12] J. P. Perdew, K. Burke, and M. Ernzerhof, *Phys. Rev. Lett.* **77**, 3865 (1996), URL <http://link.aps.org/doi/10.1103/PhysRevLett.77.3865>.
- [13] M. Shishkin, M. Marsman, and G. Kresse, *Phys. Rev. Lett.* **99**, 246403 (2007), URL <http://link.aps.org/doi/10.1103/PhysRevLett.99.246403>.

- [14] M.-Y. Liu, Q.-Y. Chen, C. Cao, and Y. He, *Phys. Chem. Chem. Phys.* **21**, 2899 (2019), URL <http://dx.doi.org/10.1039/C8CP06391E>.
- [15] B. Rasche, G. Seifert, and A. Enyashin, *The Journal of Physical Chemistry C* **114**, 22092 (2010), <https://doi.org/10.1021/jp1081565>, URL <https://doi.org/10.1021/jp1081565>.
- [16] T. Hirahara, N. Fukui, T. Shirasawa, M. Yamada, M. Aitani, H. Miyazaki, M. Matsunami, S. Kimura, T. Takahashi, S. Hasegawa, et al., *Phys. Rev. Lett.* **109**, 227401 (2012), URL <https://link.aps.org/doi/10.1103/PhysRevLett.109.227401>.
- [17] L. Cheng, H. Liu, X. Tan, J. Zhang, J. Wei, H. Lv, J. Shi, and X. Tang, *The Journal of Physical Chemistry C* **118**, 904 (2014), <https://doi.org/10.1021/jp411383j>, URL <https://doi.org/10.1021/jp411383j>.
- [18] M. Pumera and Z. Sofer, *Advanced Materials* **29**, 1605299 (2017), <https://onlinelibrary.wiley.com/doi/pdf/10.1002/adma.201605299>, URL <https://onlinelibrary.wiley.com/doi/abs/10.1002/adma.201605299>.
- [19] *Valence Shell Electron Pair Repulsion (VSEPR) theory of Molecular Geometry* (Dover Books Inc., 2012), reprint ed.
- [20] S. Jiang, S. Butler, E. Bianco, O. D. Restrepo, W. Windl, and J. E. Goldberger, *Nature Communications* **5**, 3389 (2013), URL <https://doi.org/10.1038/ncomms4389>.
- [21] A. L. Rosa, E. N. Lima, R. B. Pontes, T. Schmidt, and T. Frauenheim (2019).
- [22] A. D. Becke and K. E. Edgecombe, *J. Chem. Phys.* **92**, 53975403 (1990), URL <https://aip.scitation.org/doi/10.1063/1.458517>.